

## Characterization and reactivity of Ru/single oxides catalysts for the syngas reaction

Pérez-Zurita M. Josefina<sup>a,b,1,\*</sup>, Dufour Muriel<sup>a</sup>, Halluin Yann<sup>a</sup>,  
Griboval Anne<sup>a</sup>, Leclercq Lucien<sup>a</sup>, Leclercq Ginette<sup>a</sup>, Goldwasser Mireya<sup>b</sup>,  
Cubeiro M. Luisa<sup>b</sup>, Bond Geoffrey<sup>c</sup>

<sup>a</sup>Laboratoire de Catalyse Hétérogène et Homogène, Université des Sciences et Technologies de Lille, 59655 Villeneuve D'ascq, Cedex, France

<sup>b</sup>Facultad de Ciencias, Escuela de Química, Universidad Central de Venezuela, Apartado Postal 47102, Caracas, Venezuela

<sup>c</sup>Chemistry Department, Brunel University, Uxbridge, Middlesex UB83PH, UK

Received 15 March 2004; received in revised form 8 July 2004; accepted 9 July 2004

Available online 25 August 2004

### Abstract

A series of ruthenium-supported catalysts were prepared and characterised to determine the effect of support interaction in the production of higher alcohol from syngas. Single oxides with various degrees of acidity/reducibility such as MoO<sub>3</sub>, ZrO<sub>2</sub>, WO<sub>3</sub> and TiO<sub>2</sub> were used as supports. Al<sub>2</sub>O<sub>3</sub> was used as reference.

XPS and TGA results indicated that, on the studied supports, partial reduction to various extents was attained. The reduction of these supports was very different: while no reduction was observed for Al<sub>2</sub>O<sub>3</sub>, TiO<sub>2</sub> and ZrO<sub>2</sub>, WO<sub>3</sub> was little reduced. MoO<sub>3</sub> being the most reduced support.

Catalytic tests indicate that the selectivity towards oxygenates seems to be linked to the reducibility of the support, since with non-easily reducible oxides (Al<sub>2</sub>O<sub>3</sub>, ZrO<sub>2</sub> and TiO<sub>2</sub>) the alcohol production was very low, while higher selectivity was obtained on WO<sub>3</sub> and especially on MoO<sub>3</sub>, the reducible oxides. A SMSI effect is invoked.

© 2004 Published by Elsevier B.V.

**Keywords:** Ruthenium; CO hydrogenation; Syngas; XPS

### 1. Introduction

Ruthenium is well known as a very active catalyst for the hydrogenation of CO to hydrocarbons [1–4]. However, there is a clear suggestion from the literature that it is possible to modify its behaviour to encourage the formation of higher alcohol (C<sub>2</sub><sup>+</sup>) [4–6]. Hedrick et al. [6] reported an exceptionally high activity and selectivity for C<sub>2</sub> oxygenates in the CO/H<sub>2</sub> reaction for rhodium and ruthenium catalysts. They concluded that optimization of C<sub>2</sub> oxygenates activity and selectivity requires a proper balance between CO dissocia-

tion activity, CO insertion activity and hydrogenation activity.

Three possible ways of metal modification can be found in the literature: (i) epitaxial growth of small metal particles on reducible supports [7], (ii) decoration of large metal particles with the reducible support [8–10] and (iii) expansion of the lattice parameters of the metal due to diffusion of support species into the metal particle [11].

While the use of promoters has received much attention [8,12–20], the effect of support has been scarcely discussed for ruthenium catalysts [7,21,22]. Jackson et al. [7] studied the effect of using molybdenum and tungsten trioxides as supports for the medium pressure (1.01 MPa) hydrogenation of carbon monoxide over group VIII metals. All metals tested, except iron, showed enhancement of the activity up to two orders of magnitude when either molybdenum or

\* Corresponding author. Tel. +58 12 6051231; fax: +58 12 6051220.

E-mail address: [marperez@reacciun.ve](mailto:marperez@reacciun.ve) (P.M. Josefina).

<sup>1</sup> On leave from Universidad Central de Venezuela.

tungsten trioxide replaced silica as the support. Their results suggested that there was fast spillover/reverse spillover of hydrogen between metal and support and that this process allowed an increased effective hydrogen concentration to the reactive intermediates and hence caused an enhancement of the rates. Morris et al. [21] reported that the choice of support strongly affects the product distribution; however, they stated that the SMSI effect cannot influence catalyst behaviour in CO hydrogenation and that high activity and selectivity to higher hydrocarbons was the result of an increase in the concentration of active sites for chain propagation. Regarding the effect of dispersion, they reported that particle size plays only a minor role in the determination of catalysts behaviour in comparison with support effect and that the source of the metal and impurities from the choice of precursor can be rejected as the possible cause of differences in selectivity. Changes of morphology of the ruthenium metal particles in presence of CO were also related to the support [22]. Extended X-ray absorption fine structure (EXAFS) and IR studies were performed on ruthenium catalysts supported on  $\text{Al}_2\text{O}_3$ ,  $\text{MgO}$ ,  $\text{SiO}_2$  and  $\text{TiO}_2$  to elucidate the mechanism of the CO adsorption-induced disruption of metal clusters. EXAFS results show that after reduction, ruthenium atoms existed on all supports as small metal clusters, but the particle sizes and metal–support interactions vary with the support. CO adsorption onto  $\text{Ru}/\text{Al}_2\text{O}_3$  and  $\text{Ru}/\text{MgO}$  led to the disruption of Ru–Ru bonds while no evidences of disruption of ruthenium clusters by CO adsorption was obtained in  $\text{Ru}/\text{SiO}_2$  and  $\text{Ru}/\text{TiO}_2$ .

This paper is part of a series which describes the studies carried out on ruthenium-based catalysts; the aim of this work was to examine the effect of support interactions on the properties of ruthenium in Fischer–Tropsch catalysis for the production of higher alcohol, and to shed some light on the way this modification occurs. Since such effects are believed to occur via partial reduction of the support, a series of catalyst were prepared using single oxides with various degrees of reducibility:  $\text{MoO}_3$ ,  $\text{ZrO}_2$ ,  $\text{WO}_3$  and  $\text{TiO}_2$ .  $\text{Al}_2\text{O}_3$  was used as reference.

## 2. Experimental

### 2.1. Catalysts preparation and characterization

The catalysts were prepared by impregnation of the supports with an aqueous solution of  $\text{RuCl}_3 \cdot \text{H}_2\text{O}$  to obtain a nominal content of 1 wt.% ruthenium. After solvent evaporation, the solids were dried at  $120^\circ\text{C}$  overnight. Due to the low surface area of commercially available  $\text{MoO}_3$  and  $\text{WO}_3$  ( $\sim 3 \text{ m}^2/\text{g}$ ), these supports were synthesised using methods reported in the literature [23,24]. The  $\text{ZrO}_2$  used was Rhone Poulanc and the  $\text{Al}_2\text{O}_3$  and  $\text{TiO}_2$  were Degussa type C and P-25, respectively. Hereafter the catalysts will be denoted  $\text{Ru}/\text{X}$ , where X is the metal in the oxide support, for example,  $\text{Ru}/\text{Al}_2\text{O}_3$  will be  $\text{Ru}/\text{Al}$ .

Catalysts and supports were characterised by Chemical analyses, X-ray diffraction, Surface Area measurements, TGA in flowing  $\text{H}_2$ , XPS and CO and  $\text{H}_2$  chemisorption. The analysis of ruthenium was performed by ICP. The chlorine analysis was followed by potentiometric titration with  $\text{AgNO}_3$  and the sodium content was measured by atomic emission. XRD analysis was carried out using SIEMENS D5000 equipment in a reducing environment ( $\text{H}_2$ , 3 L/h) at room temperature. A single point BET QUANTASORB JR. apparatus measured the surface areas. Thermogravimetric analysis under  $\text{H}_2$  flow ( $\text{H}_2/\text{Ar} = 3 \text{ L/h}$ ), was performed by a SARTORIUS Electronic Balance. The temperature was raised up to  $350^\circ\text{C}$  at  $150^\circ\text{C/h}$ . XPS measurements were conducted in a LEYBOLD HERAEUS equipment provided with aluminium source ( $K\alpha$  1486.6 eV). All the catalysts were studied before and after reduction. The reduction treatments were conducted in situ using a 6%  $\text{H}_2/\text{N}_2$  mixture as reducing agent and were left overnight at  $350^\circ\text{C}$ . The samples were prepared by deposition of an alcohol suspension of the sample on a gold foil. The chemisorption measurements were carried out in a glass volumetric system. The catalysts were placed into the reactor and reduced in flowing hydrogen at  $350^\circ\text{C}$  for 3 h. After that time, the sample was outgassed at  $350^\circ\text{C}$  overnight under  $1.3 \times 10^{-7} \text{ kPa}$  pressure. After cooling at room temperature, the adsorption measurements were conducted. From the chemisorption measurements the approximate crystallite size was calculated assuming cubic crystallites, using the formula given by Smith and Everson [25]:  $\text{size } l = 6/S_m\rho$ , where  $S_m$  is the metal surface area and  $\rho$  its density =  $12.2 \text{ g/cm}^3$  and the method reported by Dalla Betta.

### 2.2. Catalytic activity measurements

The catalytic tests were performed in a stainless steel continuous fixed-bed flow micro-reactor at 5 MPa,  $\text{VVH} = 6000 \text{ h}^{-1}$ ,  $\text{H}_2/\text{CO} = 2$  and 5%  $\text{N}_2$  as internal standard.

After reduction for 3 h in flowing  $\text{H}_2$  at  $350^\circ\text{C}$  and atmospheric pressure, the catalysts were cooled to the reaction temperature ( $200\text{--}300^\circ\text{C}$ ), the pressure was increased in  $\text{H}_2$  flow up to 5 MPa and finally the feed mixture was shifted to syngas. The analyses of the reaction products were carried out on line by a gas chromatograph equipped with TCD and FID detectors and CTR-1 and Tenax columns, respectively. The activity and selectivity were determined based on CO consumption.

## 3. Results and discussion

Chemical analysis and surface area results are shown in Table 1. The percentage of ruthenium on the supports was slightly lower than the expected 1% (w/w) value, probably due to the presence of water in the hygroscopic precursor salt. The chlorine content roughly corresponds to  $\text{RuCl}_3$ . The

Table 1  
Surface area and chemical analyses

Catalyst	Ru (%)	Cl (%)	Me (%)	SA (m <sup>2</sup> /g)
Ru/Mo	1.07	0.82	66.3	12
Ru/W	0.85	0.70	77.0	15
Ru/Ti	0.80	1.05	58.4	48
Ru/Zr	0.90	1.00	67.0	60
Ru/Al	0.70	1.20	53.0	110

Me: Mo, W, Ti, Zr, Al.

surface area of the catalysts was approximately the same as those of the supports.

For all catalysts, the only diffraction pattern obtained was that of the support. The absence of ruthenium lines is not surprising taking in consideration the low ruthenium content. The diffraction patterns of MoO<sub>3</sub> and WO<sub>3</sub> supports show the presence of both oxides poorly crystallized while that of ZrO<sub>2</sub> exhibited a well-defined pattern, which evidenced a mixture of monoclinic and cubic phases.

TGA results are shown in Table 2. TGA curves show, in all cases, two consecutive weight losses were recorded: a first weight loss between room temperature and around 100 °C attributed to water elimination and a second weight loss between 100 and 350 °C attributed to chloride and oxygen elimination. The global oxide formula reported in Table 2 was calculated assuming complete reduction of ruthenium into metal and complete loss of chlorine from the surface of the catalysts.

The observed weight loss due to reduction for each catalyst was different. While for Ru/Al and Ru/Ti the weight loss corresponded to complete reduction of ruthenium, for Ru/W and Ru/Mo it was consistently beyond that which would correspond to the reduction of RuCl<sub>3</sub> (around 1%) meaning that these supports were partially reduced. The extent of reduction, however, was very different. MoO<sub>3</sub> was the most reduced support, being the weight loss consistent with total reduction of ruthenium into metal and reduction of MoO<sub>3</sub> to MoO<sub>2</sub>. After reduction, the sample shows the dark blue colour characteristic of MoO<sub>2</sub>. The degree of reduction of WO<sub>3</sub> was intermediate.

For Ru/Zr the results show a slightly higher weight loss than expected. ZrO<sub>2</sub> is a very stable oxide and cannot be reduced at temperatures lower than 400 °C; besides, it is well known that because Zr-carbonate formation, its pur-

Table 2  
Weight loss and final formula

Catalyst	Weight loss (%) T <sup>a</sup> (25–100)	Weight loss (%) T <sup>a</sup> (100–350)	Total weight loss (%)	Catalyst formula
Ru/Mo	4.1	13.0	17.1	Ru/MoO <sub>1.90</sub>
Ru/W	4.8	3.9	8.7	Ru/WO <sub>2.66</sub>
Ru/Ti	4.2	1.2	5.4	Ru/TiO <sub>2</sub>
Ru/Zr	4.7	1.4	6.1	Ru/ZrO <sub>1.95</sub>
Ru/Al	7.5	0.6	8.1	Ru/Al <sub>2</sub> O <sub>3</sub>

<sup>a</sup> Range of temperature (°C).

ification is difficult. Consequently, the weight loss observed could probably be attributed to carbonate decomposition rather than to partial reduction of the ZrO<sub>2</sub> support.

XPS confirmed the partial reduction of MoO<sub>3</sub> and WO<sub>3</sub> supports observed by TGA analyses. For WO<sub>3</sub>, the valley between the W4f<sub>5/2</sub> and W4f<sub>7/2</sub> signals was higher in the reduced sample than in the unreduced solid, revealing partial reduction of WO<sub>3</sub>. Nevertheless, the position of the two maxima was not modified, indicating a modest reduction. On the contrary, the position of the Mo3d<sub>5/2</sub> signal shifted after reduction and changed from 233.1 eV characteristic of Mo<sup>6+</sup> in MoO<sub>3</sub> to 230 eV characteristic of Mo<sup>4+</sup> probably as MoO<sub>2</sub>, in agreement with the thermogravimetric analysis.

XPS also evidenced the presence of Zr-carbonate discussed above, as carbon from carbonate species was observed into the C 1s peak at 285 eV confirming that the slight weight loss observed for ZrO<sub>2</sub> could be clearly related to the presence of Zr-carbonate which decomposed under hydrogen atmosphere, as previously discussed.

In all cases, on the unreduced catalysts, the BE corresponding to the Ru 3d<sub>5/2</sub> level was close to 282 eV characteristic of Ru<sup>3+</sup> in RuCl<sub>3</sub>. For the reduced catalysts, the value of 280 eV obtained for the BE of Ru 3d<sub>5/2</sub> signal indicates that ruthenium was reduced to ruthenium metal.

XPS intensity ratios of metal particle related peaks  $I_p$  and support related peaks  $I_s$  are strongly dependent on metal dispersion [26]. However, the existing models for applying this statement, rest on assumptions that have restrictions when used on real catalysts. The most expanded model is that proposed by Kirkhof and Mouljijn [27] who considered the catalysts as a series of slabs with cubic particles of sizes  $c$  in between and take into account the textural properties of the support, i.e. surface area and porosity.

In our case, the  $(I_{Ru}/I_{Me})$  values cannot be used directly to assess the dispersion of ruthenium since the surface areas of the supports are very different. Consequently, we have calculated particle sizes from Kirkhof and Mouljijn [27] equation which give a more realistic result.

Particle size was calculated using a simplified Kirkhof–Mouljijn formula [27]:

$$\left(\frac{I_{Ru}}{I_{Me}}\right)_{\text{exp}} = \left(\frac{I_{Ru}}{I_{Me}}\right)_{\text{monolayer}} \left[\frac{1 - e^{-\alpha}}{\alpha}\right] \quad (1)$$

$$\alpha = \frac{c}{\lambda_{pp}} \quad (2)$$

where  $(I_{Ru}/I_{Me})_{\text{exp}}$  is the experimental electron intensity ratio,  $c$  is the ruthenium particle size,  $\lambda_{pp}$  is the inelastic mean free path (IMFP) of the Ru<sub>3d</sub> photoelectron escaping through the metal,  $(I_{Ru}/I_{Me})_{\text{monolayer}}$  is the predicted electron intensity ratio assuming monolayer coverage of the support by ruthenium.  $(I_{Ru}/I_{Me})_{\text{monolayer}}$  was obtained according to equation [3]:

$$\left(\frac{I_{Ru}}{I_{Me}}\right)_{\text{monolayer}} = \left(\frac{n_{Ru}}{n_{Me}}\right)_{\text{bulk}} \left(\frac{\sigma_{Ru}}{\sigma_{Me}}\right) \left(\frac{\beta_1}{2}\right) \left[\frac{1 + e^{-\beta_1}}{1 - e^{-\beta_1}}\right] \quad (3)$$

where  $(n_{\text{Ru}}/n_{\text{Me}})_{\text{bulk}}$  is the ratio of bulk atomic concentration,  $\sigma_{\text{Ru}}$  and  $\sigma_{\text{Me}}$  are the photoelectron cross-sections reported by Scofield [28],  $\beta_1 = t/\lambda_{\text{ss}}$ ;  $\beta_2 = t/\lambda_{\text{ps}}$  and  $t$  is the thickness of the slabs and is estimated from the density  $\rho$  and the specific surface area  $S_o$  of the support  $t = 2/\rho S_o$ . Table 3 shows the results obtained.

Table 3 shows the results obtained. The smallest particle size was obtained for Ru/Ti catalyst while the biggest corresponded to Ru/Al. Ru/Mo and Ru/W catalysts showed a rather large particle size which goes in line with the fact that, for a given degree of dispersion and similar ruthenium loading, ruthenium should be less dispersed on low surface area supports. From this result it follows that the order of dispersion from XPS result is:

$$\frac{\text{Ru}}{\text{Ti}} > \frac{\text{Ru}}{\text{Zr}} > \frac{\text{Ru}}{\text{Mo}} > \frac{\text{Ru}}{\text{W}} > \frac{\text{Ru}}{\text{Al}}$$

The fact that Ru/Mo and Ru/W exhibited a similar dispersion as Ru/Al although its surface area is smaller could be explained taking into consideration the low value of the isoelectric point of both supports, which favours a better interaction between  $\text{MoO}_3$  and  $\text{WO}_3$  with the ruthenium species. On the other hand, it has been reported [1,22] that the interaction of ruthenium with alumina is very weak leading to ruthenium sintering.

For most catalysts, the ratio  $n_{\text{O}}/n_{\text{Me}}$  in the surface decreases when the catalysts were reduced. However, this ratio strongly decreases in the case of Ru/Mo and, to a lesser extent, in the case of Ru/W, providing further evidence of the support reduction taking place on both catalysts under the studied conditions.

It is observed that  $\text{ZrO}_2$  and  $\text{Al}_2\text{O}_3$  supports retain chlorine after the reduction process, while  $\text{TiO}_2$ ,  $\text{MoO}_3$  and  $\text{WO}_3$  did not. This corroborates the exchange of  $\text{OH}^-$  by  $\text{Cl}^-$ , by means of a chemical reaction between surface hydroxyl groups of the supports and chloride species in solution during the impregnation process, widely referred in the literature.

Table 4 shows the CO and  $\text{H}_2$  chemisorption results. It is clear that the hydrogen uptake was rather low for all catalysts. Consequently, the ruthenium dispersion, calculated based on  $\text{H}_2$  uptake, was poor. On the contrary, the amount of CO chemisorbed was tremendously high. Similar discrepancies between  $\text{H}_2$  and CO uptakes could be found in the literature and explanations varies as different processes could be taking place: (i) more than one CO could be adsorbed per ruthenium atom forming polycarbonyl species; (ii) CO can be adsorbed on the O vacancies formed on partially reduced supports (iii) the CO chemisorption could lead to ruthenium redispersion, or (iv) the  $\text{H}_2$  chemisorption could be a kinetically activated process. In all these cases the amount of adsorbed  $\text{H}_2$  could be smaller than that corresponding to one hydrogen atom per surface metal atom [13,16,29–32]. In our case, the order of CO uptake follows the same trend as the reducibility obtained by TGA and XPS analyses, i.e.  $\text{Ru/Mo} > \text{Ru/Zr} > \text{Ru/Ti} > \text{Ru/Al}$ . This result seems to indicate that the O vacancies formed on the supports act as CO chemisorption sites. However, in complex systems such as these, a combination of several of the above mentioned processes could take place.

The reason why Ru/W did not chemisorbs either hydrogen or CO at low pressure and room temperature is probably due to a partial covering of ruthenium particles by  $\text{W}^{x+}$  species that prevent chemisorption. The presence of Na coming from the support synthesis could also play an important role by either, covering the ruthenium particles or promoting sintering.

At higher reduction temperatures, Ru/Zr doubled the amount of chemisorbed hydrogen while the CO chemisorption is reduced to half. In general, an increase in the amount of chemisorbed hydrogen after treatment at a higher temperature is explained in terms of a completed reduction of the metal (which was not completely reduced at the lower temperature) or due to the presence of adsorbed species which could inhibit hydrogen chemisorption. In the first case, it is clear that, as the amount of metallic ruthenium

Table 3  
XPS semi-quantitative analysis

Catalyst	$(n_{\text{Ru}}/n_{\text{Me}})_{\text{bulk}}$	$(I_{\text{Ru}}/I_{\text{Me}})_{\text{exp}}$	$(I_{\text{Ru}}/I_{\text{Me}})_{\text{monolayer}}$	Particle size (nm)	$n_{\text{O}}/n_{\text{Me}}^{\text{a}}$	$n_{\text{Cl}}/n_{\text{Ru}}^{\text{a}}$
Ru/Mo <sup>b</sup>	0.014	0.054	0.066	11.5	3.41	2.20
Ru/Mo <sup>c</sup>		0.058			2.07	–
Ru/W <sup>b</sup>	0.020	0.096	0.060	12.3	3.50	2.90
Ru/W <sup>c</sup>		0.044			3.22	–
Ru/Ti <sup>b</sup>	0.006	0.037	0.014	8.4	1.79	2.41
Ru/Ti <sup>c</sup>		0.024			1.82	–
Ru/Zr <sup>b</sup>	0.012	0.030	0.021	10.0	2.21	2.45
Ru/Zr <sup>c</sup>		0.026			2.20	1.46
Ru/Al <sup>b</sup>	0.004	0.063	0.061	12.6	1.63	5.45
Ru/Al <sup>c</sup>		0.042			1.57	2.24

<sup>a</sup> Atomic ratios in the surface layers from the integrated intensities using the equation:  $(n_i/n_j)_{\text{XPS}} = (I_i/I_j)(\sigma_i/\sigma_j)(KE_j/KE_i)^{a+1}$ ; KE = kinetic energy.

<sup>b</sup> Dried.

<sup>c</sup> Reduced—measure the asymmetry Me: Zr, W, Mo, Ti, Al.

Table 4  
CO and H<sub>2</sub> chemisorption

Catalyst	H <sub>2</sub> (μmol/g <sub>cat</sub> )	CO (μmol/g <sub>cat</sub> )	D (H <sub>2</sub> ) <sup>a</sup> (%)	D (CO) <sup>b</sup> (%)	Particle size [39] (nm)
Ru/Mo	5.5	280	11	380	9.4
Ru/W	0.0	Low	–	–	–
Ru/Ti	8.5	100	17	100	6.1
Ru/Zr	6.0	185	12	185	8.6
Ru/Al	2.0	53	4	53	25.9
Ru/Zr <sup>c</sup>	11	99	22	99	4.7
Ru/Zr <sup>d</sup>	11	96	22	96	4.7
ZrO <sub>2</sub>	0.0	20	–	–	–

<sup>a</sup> Stoichiometry: 0.5.

<sup>b</sup> Stoichiometry: 1.

<sup>c</sup> T<sub>red</sub> = 400 °C.

<sup>d</sup> T<sub>red</sub> = 450 °C.

increase, the H<sub>2</sub> chemisorption increase. Since our TGA and XPS results show complete reduction of ruthenium in Ru/Zr, the above mentioned phenomenon cannot explain the observed increase of hydrogen uptake. On the contrary, the presence of adsorbed species could give a fair explanation. As mentioned before, ZrO<sub>2</sub> support is likely to contain some Zr-carbonate that could decompose to carbonaceous species at 350 °C and desorbs at higher temperatures. Also, the XPS results show that chloride was retained on the zirconia support after the reduction treatment. These adsorbed species (either carbonaceous or chloride species) could inhibit hydrogen adsorption or interrupt the ensemble of metal atoms as to produce a kinetic effect.

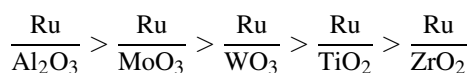
The reduction in half of the amount of CO chemisorbed on zirconia catalysts after reduction at a higher temperature could be attributed to dispersion. Rieck and Bell [33] reported that, as the dispersion decrease, the ratio of linearly held CO to bridge-bonded CO decreases.

Particle size calculated from H<sub>2</sub> chemisorption is also reported in Table 4. A good agreement was obtained with the results reported in Table 3. The observed trend of dispersion obtained with XPS was confirmed by hydrogen chemisorption.

### 3.1. Catalytic activity measurements

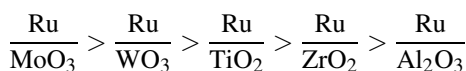
Under the experimental conditions used, the supports alone showed that they were almost inactive for syngas conversion. Only traces of C<sub>1</sub>–C<sub>3</sub> hydrocarbons were detected.

Table 5 show the catalytic behaviour for all Ru/support catalysts. According to their activity, the catalysts can be ordered as follows:



The observed activity trend seems to be related to the acidity of the supports. Since Lewis acid sites are directly related to Pauling electronegativity [34,35], the decreasing order of

acidity in our system is:



The observed trend in both series is almost identical, with the only exception of Ru/Al which is the most active and also the less acid catalyst.

Boffa et al. [34] studied rhodium over different oxides and proposed that the effect of metal oxide promotion on the rate of CO and CO<sub>2</sub> hydrogenation could be attributed to the formation of Lewis acid–base complexes between adsorbed CO or CH<sub>x</sub>O at the boundary between the metal oxide and the exposed metal surface which are envisioned to weaken the CO bond and facilitate its dissociation.

In Ru/Al, particle size could be playing an important role. The XPS and hydrogen chemisorption results show that Ru/Al had the biggest particle size. Rick and Bell [33] shown that dispersion has an effect on the interaction of hydrogen and CO with Pd/SiO<sub>2</sub>. The authors reported that the ratio of linearly bonded CO to bridge bonded CO decrease with dispersion and concluded that CO dissociation occurs preferentially at the bridge bonded CO sites and proceeds more readily as dispersion decrease.

Some differences in product distribution were observed depending on the support. The main products were alkanes, with CH<sub>4</sub> as major product. The highest C<sub>5</sub><sup>+</sup> selectivity was obtained on Ru/Ti, with the lowest methane production.

Table 5  
CO hydrogenation reaction

Catalyst	X <sub>CO</sub> (%)	S <sub>CO2</sub> (%)	S <sub>CH4</sub> (%)	S <sub>C2–C4</sub> (%)	S <sub>C5+</sub> (%)	S <sub>Oxy</sub> (%)	Y <sub>Oxy</sub> (%)
Ru/Mo	16.2	8.1	41.8	33.1	5.3	11.7	1.90
Ru/W	15.2	1.2	51.9	30.7	15.3	0.9	0.14
Ru/Ti	4.5	0.2	23.2	37.6	39.0	0.0	0.0
Ru/Zr	1.9	0.0	42.1	37.8	19.8	0.3	0.01
Ru/Al	25.8	0.0	44.8	33.4	21.8	0.0	0.0

T = 240 °C; P = 5 MPa, VVH = 6000 h<sup>-1</sup>, time on stream = 24 h, H<sub>2</sub>/CO = 2; yield (Y) = SX<sub>CO</sub>.

Table 6  
CO hydrogenation on reducible supports: oxygenate distribution

Catalyst	Ru/WO <sub>3</sub>			Ru/MO <sub>3</sub>		
	220 °C (61–66 h)	240 °C (69–76 h)	260 °C (27–47 h)	205 °C (26–43 h)	240 °C (0–20 h)	260 °C (45–50 h)
X <sub>CO</sub> (%)	3.7	5.0	14.3	9.1	16.2	31.7
S <sub>CO<sub>2</sub></sub> (%)	0.0	0.0	0.5	8.5	8.1	9.6
S <sub>Oxy</sub> <sup>a</sup> (%)	5.4	3.0	0.0	35.6	12.0	2.0
Y <sub>Oxy</sub> (%)	0.20	0.15	0.0	3.24	1.90	0.63
Alcohol distribution <sup>a</sup>						
S <sub>C<sub>1</sub>OH</sub> (%)	1.4	3.4	0.0	30.5	10.7	1.9
S <sub>C<sub>2</sub>OH</sub> (%)	1.3	1.5	0.0	4.2	1.0	0.4
S <sub>C<sub>3</sub>OH</sub> (%)	0.3	0.5	0.0	0.9	0.3	0.1

1 mL catalyst; H<sub>2</sub>/CO = 2; VVH = 6000 h<sup>-1</sup>; T<sub>red</sub> = 350 °C; yield(Y) = SX<sub>CO</sub>.

<sup>a</sup> CO<sub>2</sub> free.

Selectivity to oxygenate seems to be related to the reducibility of the support. Ru/Mo gave the highest proportion of alcohols, which in turn was the catalyst with the more reducible support. This result could be explained in two possible ways. Either a SMSI effect could maximize the amount of the pair Ru<sup>0</sup>–Ru<sup>x+</sup> species by electron transfer from ruthenium towards the support involving a two site mechanism or as stated in an earlier work [8], the surface of ruthenium particles is partially covered by oxo-Mo species in a way that maximises the Ru–Mo pair sites which in turn are proposed to be responsible for oxygenate formation.

Selectivity towards oxygenate seems also be related to metal dispersion. The XPS and chemisorption results, showed a decreasing order of dispersion which follows the same pattern as oxygenate selectivity. A good dispersion should produce a more efficient metal–support contact which in turn will provide a greater number of Ru–Mo sites. This observation was also reported by Gotti and Prins [36] whom observed that a more efficient promotion for methanol from syngas is found when dispersion is higher due to a greater promoter–metal contact area for catalysts with small noble metal particles. More recently, Hiroki et al. [37] reported on highly dispersed Fe/SiO<sub>2</sub> catalysts prepared using a microemulsion preparation method for CO hydrogenation, and found extremely high selectivity (>40 C mol%) for C<sub>2</sub>+ oxygenates. Whether the reducibility of the support plays a role on the dispersion of the final catalysts and both characteristics are needed for having high oxygenate yield in ruthenium based catalysts seems quite possible.

For a given reaction temperature, conversion in all cases were very dissimilar. This fact does not permit a fair comparison among the catalysts studied. The expected tendency to a decrease in the selectivity to oxygenate with an increase in conversion was observed. With the aim to overcome this problem, oxygenate yields were also reported in Table 5.

Since the thermodynamics of the reaction predicts that the selectivity of oxygenate products are likely to be higher at low temperature and high pressure, Table 6 shows the effect of temperature on the alcohol selectivity and its

distribution. This tendency is clearly shown for Ru/MoO<sub>3</sub> where an increase in temperature from 205 to 260 °C, decreases alcohol selectivity from 35.6 to 2.0.

Among the studied catalysts, the best alcohol selectivity was obtained for Ru/MoO<sub>3</sub> with up to 36% of alcohol in the products. It is interesting to point out that, on this catalyst, the higher selectivity to CO<sub>2</sub> was obtained, which could be related to the water gas shift reaction (WGS). As one of the proposed mechanisms for the WGS is a redox process favoured over reducible oxides [38], this catalyst may have future applications for this reaction as well as other reactions catalyzed by metals interacting with Lewis acid sites.

#### 4. Conclusions

The results obtained showed that support interactions can transform ruthenium from an alkane producing metal when deposited on a non-reducible support to an oxygenate producing catalyst when supported on a partially reducible oxide. The catalytic tests indicated that the selectivity of ruthenium supported on single oxides for the formation of oxygenates, seems to be linked to the reducibility of the support since with non-easily reducible supports (ZrO<sub>2</sub>, TiO<sub>2</sub> and Al<sub>2</sub>O<sub>3</sub>) the alcohol production was very low. On the contrary, with WO<sub>3</sub> and especially with MoO<sub>3</sub> as supports the alcohol production was enhanced.

#### Acknowledgements

Financial support by the European Union Council (Grant No. CI1\*-CT92-0093) and FONACIT (Agenda Petróleo 00003739) are gratefully acknowledged.

#### References

- [1] H. Abrevaya, M.J. Cohn, W.M. Targos, H.J. Robota, Catal. Lett. 7 (1990) 183.

- [2] L. Gucci, R. Sundararajan, Zs. Koppány, Z. Zsoldos, Z. Schay, F. Mizukami, S. Niwa, *J. Catal.* 167 (1997) 482.
- [3] M.A. Vanice, *J. Catal.* 37 (1975) 449.
- [4] M.R. Goldwasser, M.L. Cubeiro, M.C. Da Silva, M.J. Pérez Zurita, G. Leclercq, L. Leclercq, M. Dufour, G.C. Bond, *Stud. Surf. Sci. Catal.* 107 (1997) 15.
- [5] L.E.Y. Nonneman, V. Ponc, *Catal. Lett.* 7 (1990) 197.
- [6] S.A. Hedrick, S.S.C. Chuang, A. Pant, A.G. Dastidar, *Catal. Today* 55 (3) (2000) 247.
- [7] S.D. Jackson, B.J. Brandreth, D. Winstanley, *J. Appl. Catal.* 27 (1986) 325.
- [8] M.J. Pérez Zurita, I.S. Henriquez, M.R. Goldwasser, M.L. Cubeiro, G.C. Bond, *J. Mol. Catal.* 88 (1994) 213.
- [9] J. Cunningham, S. O'Brien, J. Sanz, J.M. Rojo, J. Soria, J.L.G. Fierro, *J. Mol. Catal.* 57 (1991) 397.
- [10] J.S. Rieck, A.T. Bell, *J. Catal.* 99 (1986) 278.
- [11] L. Kepínski, M. Wolcyrz, *Appl. Catal.* 150 (1997) 197.
- [12] M. Inoue, T. Miyake, Y. Takegami, T. Inui, *Appl. Catal.* 11 (1984) 103.
- [13] A. Guerrero-Ruiz, A. Sepúlveda-Escribano, I. Rodríguez-Ramos, *Appl. Catal. A: Gen.* 120 (1994) 71.
- [14] A. Juan, D.E. Damiani, *J. Catal.* 37 (1992) 77.
- [15] A. Juan, D.E. Damiani, *Catal. Today* 15 (1992) 469.
- [16] D.O. Uner, M. Pruski, B.C. Gerstein, T.S. King, *J. Catal.* 146 (1994) 530.
- [17] N. Takahashi, T. Mori, A. Miyamoto, T. Hattori, Y. Murakami, *Appl. Catal.* 22 (1986) 137.
- [18] T. Mori, A. Miyamoto, N. Takahashi, M. Fukagaya, T. Hattori, Y. Murakami, *J. Phys. Chem.* 90 (1986) 5197.
- [19] H. Foley, A.J. Hong, J.S. Brinen, L.F. Allard, A.J. Garrat-Reed, *Appl. Catal.* 61 (1990) 351.
- [20] C.H. Yang, J.G. Goodwin Jr., *React. Kinet. Catal. Lett.* 26 (1984) 453.
- [21] S.R. Morris, R.B. Moyes, P.B. Wells, R. Whyman, in: B. Imelik (Ed.), *Metal–Support and Metal–Additive Effects in Catalysis*, Elsevier, Amsterdam, 1982, p. 247.
- [22] T. Mizushima, K. Tohji, Y. Udagawa, A. Ueno, *J. Am. Chem. Soc.* 112 (1990) 7887.
- [23] A. Chemseddine, These de Doctorat, Université Pierre et Marie Currie, Paris VI, 1986.
- [24] T. Fransen, P.C. van Berge, P. Mars, *React. Kinet. Catal. Lett.* 5 (4) (1976) 445.
- [25] K.J. Smith, R.C. Everson, *J. Catal.* 99 (1986) 349.
- [26] A.M. Venezia, *Catal. Today* 77 (2003) 359.
- [27] F.P.J.M. Kerkhof, J.A. Moulijn, *J. Phys. Chem.* 83 (1979) 1612.
- [28] J.M. Scofield, *J. Electron Spect. Related Phenom.* 8 (1976) 129.
- [29] R.A. Dalla Betta, *J. Phys. Chem.* 79 (1975) 2519.
- [30] C.H. Yang, J.G. Goodwin, *React. Kinet. Catal. Lett.* 20 (1982) 13.
- [31] P. Betancourt, A. Rives, R. Hubaut, C.E. Scott, J. Goldwasser, *Appl. Catal.* 170 (1998) 307.
- [32] K. Hadjiivanov, J.C. Lavalley, J. Lamotte, F. Maugé, J. Saint-Just, M. Che, *J. Catal.* 176 (1998) 415.
- [33] J.S. Rieck, A.T. Bell, *J. Catal.* 106 (1987) 46.
- [34] A. Boffa, C. Lin, A.T. Bell, G.A. Somorjai, *J. Catal.* 149 (1994) 149.
- [35] K. Tanabe, *Solid Acids and Bases*, Academic Press, Kondansha, Tokyo, 1970.
- [36] A. Gotti, R. Prins, *Catal. Lett.* 37 (1996) 43.
- [37] H. Hiroki, L.Z. Chen, T. Tago, K. Masahiro, W. Katsuhiko, *Appl. Catal.* 231 (2002) 81.
- [38] M.S. Wainwright, D.L. Trimm, *Catal. Today* 23 (1995) 29.
- [39] R.A. Dalla Beta, *J. Catal.* 34 (1974) 57.